An Inflationary Differential Evolution Algorithm for Space Trajectory Optimization

Massimiliano Vasile, *Member, IEEE*, Edmondo Minisci, and Marco Locatelli, *Member, IEEE*

Abstract

In this paper we define a discrete dynamical system that governs the evolution of a population of agents. From the dynamical system, a variant of Differential Evolution is derived. It is then demonstrated that, under some assumptions on the differential mutation strategy and on the local structure of the objective function, the proposed dynamical system has fixed points towards which it converges with probability one for an infinite number of generations. This property is used to derive an algorithm that performs better than standard Differential Evolution on some space trajectory optimization problems. The novel algorithm is then extended with a guided restart procedure that further increases the performance, reducing the probability of stagnation in deceptive local minima.

Index Terms

Differential Evolution, Global Trajectory Optimization.

I. INTRODUCTION

Some evolutionary heuristics can be interpreted as discrete dynamical systems governing the movements of a set of agents (or particles) in the search space. This is well known for Particle Swarm Optimization (PSO) where the variation of the velocity of each particle in the swarm is defined by a control term made of a social component and a individual (or cognitive) component [1]–[4]. The social component can be interpreted as a behavior dictated by the knowledge acquired by the whole swarm of particles, while the cognitive component can be interpreted as a behavior dictated by the knowledge acquired by each individual particle.

The same principle can be generalized and extended to other evolutionary heuristics such as Differential Evolution (DE) [5]. The analysis of a discrete dynamical system governed by the heuristics generating the behavior of individuals in DE, and in Evolutionary Computation in general, would allow for a number of considerations on the

M. Vasile is with the Department of Mechanical Engineering, University of Strathclyde, James Weir Building 75 Montrose Street G1 1XJ (phone: +44-(0)141-548-4851; fax: +44-(0)141-552-5105; email: massimiliano.vasile@strath.ac.uk).

E. Minisci is with the School of Engineering, University of Glasgow, James Watt South Building, G12 8QQ, Glasgow, UK (phone: +44-141-330-8470; fax: +44-141-330-5560; email: edmondo.minisci@glasgow.ac.uk).

M. Locatelli is with the Dipartimento di Ingegneria Informatica, Universitá degli Studi di Parma, Parma, via G. P. Usberti, 181/A, 43124, Italy (email: locatell@ce.unipr.it).

evolution of the search process and therefore on the convergence properties of a global optimization algorithm. In particular, four outcomes of the search process are possible:

- Divergence to infinity. In this case the discrete dynamical system is unstable, and the global optimization algorithm is not convergent.

- Convergence to a fixed point in D. In this case the global optimization algorithm is simply convergent in D and we can define a stopping criterion. Once the search is stopped we can define a restart procedure. Depending on the convergence profile, the use of a restart procedure can be more or less efficient.

- Convergence to a limit cycle in which the same points in D are re-sampled periodically. Even in this case we can define a stopping criterion and a restart procedure.

- Convergence to a strange (chaotic) attractor. In this case a stopping criterion cannot be clearly defined because different points are sampled at different iterations.

All outcomes are generally interesting to understand the evolution process. Identifying under which conditions divergence occurs is important to properly design an algorithm, or to define the appropriate setting, in particular in the case of automatic adaptation of some key parameters. Divergence can be seen as the opposite of the intensification process and can increase diversity and exploration. The convergence to a chaotic attractor can represent an interesting case of dense random sampling of an extended region. When this happens, the algorithm repeatedly samples the same region but never re-samples the same points. This mechanism could be useful to reconstruct an extended set with a specific property (e.g. $f(x) < \varepsilon$, with f the objective function and ε a threshold).

The main interest, in this paper, is in the most commonly desired outcome: the convergence to a fixed point (see for example [6], in the context of global root finding, for methods to eliminate undesirable behaviors). The convergence to a fixed point, even different from an optimum, can be used to induce a restart of the search process with minimum waste of resources (as it will be demonstrated in this paper).

The analysis of the dynamical properties of the dynamical system associated with a particular heuristic can give some insights into the balance between global and local exploration and the volume of the search space that is covered during the search. Extensive work on the dynamics of Genetic Algorithms and general Evolutionary Algorithms can be found in the studies of Prügel-Bennett et al. [7], [8] and Beyer [9]. Non-evolutionary examples of the use of dynamical system theory to derive effective global optimization schemes can be found in the works of Sertl and Dellnitz [10].

In this paper we propose a discrete dynamical system, or discrete map, governing the evolution of a population of individuals, being each individual a point in a d-dimensional domain D. From the discrete dynamical system we derive a variant of Differential Evolution and we study its convergence properties. In particular, it is proven that, under some assumptions, the dynamics of the proposed variant of DE converges to a fixed point or to a level set. Note that, the proofs proposed in this paper considers the whole d-dimensional discrete dynamical system associated to the evolution of the population.

The theoretical results are then used to derive a novel algorithm that performs better than DE strategies *DE/rand/1/bin* and *DE/best/1/bin* [11] on some difficult space trajectory design problems. The novel algorithm is based on a

hybridization of the proposed DE variant and the logic behind Monotonic Basin Hopping (MBH) [12].

The paper is organized as follows: after introducing the dynamics of a population of agents, three convergence theorems are demonstrated. Then an inflationary DE algorithm based on a hybridization between a variant of DE and MBH is derived. A description of the test cases and testing procedure follows. After presenting the results of the tests, the search space is analyzed to derive some considerations on the general applicability of the results.

II. AGENT DYNAMICS

In this section we start by defining a generic discrete dynamical system governing the motion of an agent in a generic search space D. From this general description we derive a variant of what Storn and Price defined as the basic DE strategy [11].

If we consider that a candidate solution vector in a generic d-dimensional box,

$$D = [b_l(1) \; b_u(1)] \times [b_l(2) \; b_u(2)] \times ...[b_l(d) \; b_u(d)] \tag{1}$$

is associated to an agent, then the heuristic governing its motion in D can be written as the following discrete dynamical system:

$$\mathbf{v}_{i,k+1} = (1-c)\mathbf{v}_{i,k} + \mathbf{u}_{i,k}$$
$$\mathbf{x}_{i,k+1} = \mathbf{x}_{i,k} + \nu S(\mathbf{x}_{i,k} + \mathbf{v}_{i,k+1}, \mathbf{x}_{i,k})\mathbf{v}_{i,k+1} \tag{2}$$

with

$$\nu = \min\left(\left[v_{max}, v_{i,k+1}\right]\right)/v_{i,k+1} \tag{3}$$

The function $S(\mathbf{x}_{i,k} + \mathbf{v}_{i,k+1}, \mathbf{x}_{i,k})$ is a selection operator that can be either 1 if the candidate point $\mathbf{x}_{i,k} + \mathbf{v}_{i,k+1}$ is accepted or 0 if it is not accepted. Different evolutionary algorithms have different ways to define S.

The control $\mathbf{u}_{i,k}$ defines the next point that will be sampled for each one of the existing points in the solution space, the vectors $\mathbf{x}_{i,k}$ and $\mathbf{v}_{i,k}$ define the current state of the agent in the solution space at stage k of the search process, $\mathbf{x}_{i,k+1}$ and $\mathbf{v}_{i,k+1}$ define the state of the agent in the solution space at stage $k+1$ of the search process and c is a viscosity, or dissipative coefficient, for the process. Eq. (3) represents a limit sphere around the agent $\mathbf{x}_{i,k}$ at stage k of the search process. Different evolutionary algorithms have different ways to define $\mathbf{u}_{i,k}$, ν and c (see for example the dynamics of PSO [1]). In this paper we will focus on the way $\mathbf{u}_{i,k}$, ν and c are defined in Differential Evolution.

Now consider the $\mathbf{u}_{i,k}$ defined by:

$$\mathbf{u}_{i,k} = \mathbf{e}\left[(\mathbf{x}_{i_3,k} - \mathbf{x}_{i,k}) + F(\mathbf{x}_{i_2,k} - \mathbf{x}_{i_1,k})\right] \tag{4}$$

where i_1, i_2 and i_3 are integer numbers randomly chosen in the interval $[1, \; n_{pop}] \subset \mathbb{N}$ of indexes of the population, and $\mathbf{e}$ is a mask containing a random number of 0 and 1 according to:

$$e(j) = \begin{cases} 1 \Rightarrow r_j \leq C_R \\ 0 \Rightarrow r_j > C_R \end{cases} \tag{5}$$

with j randomly chosen in the interval $[1\ d]$, so that $\mathbf{e}$ contains at least one nonzero component, d the dimension of the solution vector, r_j a random number taken from a random uniform distribution $r_j \in U[0,1]$ and C_R a constant. The product between $\mathbf{e}$ and $[(\mathbf{x}_{i_3,k} - \mathbf{x}_{i,k}) + F(\mathbf{x}_{i_2,k} - \mathbf{x}_{i_1,k})]$ in Eq. (4) has to be intended component-wise. The index i_3 can be chosen at random (this option will be called exploration strategy in the remainder of this paper) or can be the index of the best solution vector $\mathbf{x}_{best}$ (this option will be called convergence strategy in the remainder of this paper). Selecting the best solution vector or a random one changes significantly the convergence speed of the algorithm. The selection function S can be either 1 or 0 depending on the relative value of the objective function of the new candidate individual generated with Eq. (4) with respect to the one of the current individual.

In other words the selection function S can be expressed as:

$$S(\mathbf{x}_{i,k} + \mathbf{u}_{i,k}, \mathbf{x}_{i,k}) = \begin{cases} 1 & \text{if } f(\mathbf{x}_{i,k} + \mathbf{u}_{i,k}) < f(\mathbf{x}_{i,k}) \\ 0 & \text{otherwise} \end{cases} \tag{6}$$

Note that in this paper we consider minimization problems in which the lowest value of f is sought.

If one takes $c = 1$, $\nu = 1$ and $v_{max} = +\infty$, then map (2) reduces to:

$$\mathbf{x}_{i,k+1} = \mathbf{x}_{i,k} + S(\mathbf{x}_{i,k} + \mathbf{u}_{i,k}, \mathbf{x}_{i,k})\mathbf{u}_{i,k} \tag{7}$$

In the general case the indices i_1, i_2 and i_3 can assume any value. However, if the three indexes i_1, i_2 and i_3 are restricted to be mutually different, map (7), with $\mathbf{u}_{i,k}$ defined in (4), $\mathbf{e}$ defined in (5) and S defined in (6), is the DE basic strategy *DE/rand/1/bin* defined by Storn and Price in [11]. If i_3 is taken as the index of the best individual i_{best}, and i_1, i_2 and i_3 are mutually different, then one can obtain the DE strategy *DE/best/1/bin*. In fact, if (4) is substituted in (7) one gets:

$$\mathbf{x}_{i,k+1} = (\mathbf{1} - S\mathbf{e})\mathbf{x}_{i,k} + S\mathbf{e}\left[(\mathbf{x}_{i_3,k} + F(\mathbf{x}_{i_2,k} - \mathbf{x}_{i_1,k})]\right. \tag{8}$$

Now, if the selection function does not accept the candidate point $\mathbf{x}_{i,k} + \mathbf{u}_{i,k}$, then $S = 0$, therefore (8) reduces to $\mathbf{x}_{i,k+1} = \mathbf{x}_{i,k}$ (i.e. the state of the agent remains unchanged). If the candidate point is accepted instead, then the new location of the agent is:

$$\mathbf{x}_{i,k+1} = (\mathbf{1} - \mathbf{e})\mathbf{x}_{i,k} + \mathbf{e}\left[(\mathbf{x}_{i_3,k} + F(\mathbf{x}_{i_2,k} - \mathbf{x}_{i_1,k})]\right. \tag{9}$$

The quantity in square brackets is the basic DE strategy *DE/rand/1/bin* or the variant *DE/best/1/bin*, respectively for i_3 random or $i_3 = i_{best}$. The mask $\mathbf{e}$ together with $(\mathbf{1} - \mathbf{e})\mathbf{x}_{i,k}$ represent the cross-over operator in the basic DE strategy [11], with $\mathbf{1}$ a vector of 1's and the products $\mathbf{1}\mathbf{x}_{i,k}$ and $\mathbf{e}\mathbf{x}_{i,k}$ that are both component-wise. In fact, $\mathbf{x}_{i,k+1}$ is made of the components of $\mathbf{x}_{i,k}$ that correspond to the zero elements of $\mathbf{e}$, and the components of $[(\mathbf{x}_{i_3,k} + F(\mathbf{x}_{i_2,k} - \mathbf{x}_{i_1,k})]$ that correspond to the nonzero elements of $\mathbf{e}$. If the assumption of mutually different indexes is dropped then map (7) can be seen as a further variant of the basic DE strategy.

In compact matrix form for the entire population, map (7) can be written as:

$$\mathbf{X}_{k+1} = \mathbf{J}_k \mathbf{X}_k \tag{10}$$

with the i-th line of matrix $\mathbf{X}_k \in \mathbb{R}^{n_{pop} \times d}$ is point $\mathbf{x}_{i,k}$.

To be more precise, in the case $\mathbf{x}_{i,k+1} \notin D$, then every component j violating the boundaries $\mathbf{b}_l$ and $\mathbf{b}_u$ is projected back into D by picking the new value $x(j)_{i,k+1} = b_l(j) + \varsigma(b_u(j) - b_l(j))$, where ς is taken from a random uniform distribution $\varsigma \in U[0,1]$. The interest is now in the properties of map (10). We start by observing that if $S(\mathbf{x}_{i,k} + \mathbf{u}_{i,k}, \mathbf{x}_{i,k}) = 1 \Leftrightarrow f(\mathbf{x}_{i,k} + \mathbf{u}_{i,k}) < f(\mathbf{x}_{i,k})$, for $i = 1, ..., n_{pop}$, the global minimizer $\mathbf{x}_g \in D$ is a fixed point for map (7) since every point $\mathbf{x} \in D$ is such that $f(\mathbf{x}) \geq f(\mathbf{x}_g)$.

Then, let us assume that at every iteration k we can find two connected subsets D_k and D_k^* of D such that $f(\mathbf{x}_k) < f(\mathbf{x}_k^*), \forall \mathbf{x}_k \in D_k, \forall \mathbf{x}_k^* \in D_k^* \setminus D_k$, and let us also assume that $P_k \subseteq D_k$ while $P_{k+1} \subseteq D_k^*$ (recall that P_k and P_{k+1} denote the populations at iteration k and $k+1$ respectively). If $\mathbf{x}_l$ is the lowest local minimum in D_k, then $\mathbf{x}_l$ is a fixed point in D_k for map (7). In fact, every point generated by map (7) must be in D_k and $f(\mathbf{x}_l) < f(\mathbf{x}), \forall \mathbf{x} \in D_k$.

Moreover, under the above assumptions the reciprocal distance of the individuals cannot grow indefinitely because of the map (7), therefore the map cannot be divergent.

Finally, a matrix $\mathbf{X}_k$ whose lines are n_{pop} replications of a unique point $\mathbf{x} \in D$, is always a fixed point for the map (10).

Now one can consider two variants of Differential Evolution: one in which index i_1 can be equal to index i_2 but both are different from i_3 and one in which index i_1 can be equal to index i_3 but both are different from i_2. In these cases two interesting results can be proven. First of all we prove that if i_1 can be equal to index i_2 then the population can collapse to a single point in D.

THEOREM II.1 *If, for every k, i_1 is equal to i_2 with strictly positive probability and $f(\mathbf{x}_{i_{best},k}) = f(\mathbf{x}_{i,k}) \Leftrightarrow \mathbf{x}_{i_{best},k} = \mathbf{x}_{i,k}$(i.e., the set of best points within the population is made up by a single point, multiple copies of which possibly exist),then the population collapses to a single point with probability 1 for $k \to \infty$ under the effect of the discrete dynamical system (7)*

Proof: If i_1 is equal to i_2 with strictly positive probability, and $f(\mathbf{x}_{i_{best},k}) = f(\mathbf{x}_{i,k}) \Leftrightarrow \mathbf{x}_{i_{best},k} = \mathbf{x}_{i,k}$ for every k, then map (7) at each iteration k can generate, with strictly positive probability, a displacement $\mathbf{u}_{i,k} = (\mathbf{x}_{i_3,k} - \mathbf{x}_{i,k})$ for each member i, $i = 1, \ldots, n_{pop}$. This happens if, for each $i \in [1, \ldots, n_{pop}]$, the following event, whose probability is strictly positive, occurs

$$e(s) = 1, \ \ s = 1, \ldots, d, \ \ i_3 \neq i_1 = i_2.$$

$$i_3 \in \{i \ : \ f(x_{i,k}) = f(x_{i_{best},k})\} \tag{11}$$

Then, at each iteration we have a strictly positive probability that the two or more individuals collapse into the single point $x_{i_{best},k}$ and for $k \to \infty$ the whole population collapses to a single point with probability one. ∎

After a collapse, the population cannot progress further and needs to be restarted. It is important to evaluate the probability of a total collapse, in fact if the collapse is progressive the population can keep on exploring but if the collapse is instantaneous the evolution ceases. Let us analyze the worst case in which, $i_3 = i_{best}$. Then if for

all the individuals $i_1 = i_2$ and $\mathbf{e} = 1$ we have a total instantaneous collapse. The probability of having $i_1 = i_2$ is $1/n_{pop}$ and the probability of having $n_{pop} - 1$ individuals collapsing at the same iteration k is $(1/n_{pop})^{n_{pop}-1}$. Furthermore, given a $C_R \neq 1$ the probability to have $\mathbf{e} = 1$ is C_R^{d-1}. Thus the total probability of an instantaneous total collapse is $[(1/n_{pop})C_R^{d-1}]^{n_{pop}-1}$. The event has positive but small probability to happen. The complementary probability is $1 - [(1/n_{pop})C_R^{d-1}]^{n_{pop}-1}$ and the probability to have at least one total collapse after k_h generations is $1 - \{1 - [(1/n_{pop})C_R^{d-1}]^{n_{pop}-1}\}^{k_h}$. Therefore, allowing the indexes to assume the value $i_1 = i_2$ introduces the following interesting property. If the population is stagnating, and the condition $f(\mathbf{x}_{i_{best},k}) = f(\mathbf{x}_{i,k}) \Leftrightarrow \mathbf{x}_{i_{best},k} = \mathbf{x}_{i,k}$ holds true, eventually there will be a total collapse and the population can be restarted with no risk to interrupt the evolutionary process.

If i_1 is equal to i_3 with strictly positive probability but both are always different from i_2, then convergence to a fixed point can be guaranteed if the function f is strictly quasi-convex [13] in D, and D is compact and convex. In other words, under the given assumptions, the population will converge to a single point. We immediately remark that such point is not necessarily a local minimizer of the problem.

LEMMA II.2 *Let f be a continuous and strictly quasi-convex function on a set D and let us assume that D is compact, convex and is not a singleton. Then, the following minimization problem with $F \in (0,1)$ has a strictly positive minimum value $\delta_r(\epsilon)$ for ϵ small enough:*

$$
\begin{aligned}
\delta_r(\epsilon) = \quad &\min \quad g(\mathbf{y}_1, \mathbf{y}_2) = f(\mathbf{y}_2) - f(F\mathbf{y}_1 + (1-F)\mathbf{y}_2) \\
&s.t. \quad \mathbf{y}_1, \mathbf{y}_2 \in D \\
&\qquad \|\mathbf{y}_1 - \mathbf{y}_2\| \geq \epsilon \\
&\qquad f(\mathbf{y}_1) \leq f(\mathbf{y}_2)
\end{aligned}
\tag{12}
$$

Proof:

Since f is strictly quasi-convex $g(\mathbf{y}_1, \mathbf{y}_2) > 0$, $\forall \mathbf{y}_1, \mathbf{y}_2 \in D$; furthermore, the feasible region is nonempty (if ϵ is small enough and D is not a singleton) and compact. Therefore, according to Weierstrass' theorem the function g attains its minimum value over the feasible region. If we denote by $(\mathbf{y}_1^*, \mathbf{y}_2^*)$ a global minimum point of the problem, then we have

$$
\delta_r(\epsilon) = g(\mathbf{y}_1^*, \mathbf{y}_2^*) > 0.
\tag{13}
$$

∎

THEOREM II.3 *Assume that index i_1 can be equal to i_3. Given a function f that is strictly quasi-convex over the compact and convex set D, and a population $P_k \in D$, then if $F \in (0,1)$ and $S(\mathbf{x}_{i,k} + \mathbf{u}_{i,k}, \mathbf{x}_{i,k}) = 1 \Leftrightarrow f(\mathbf{x}_{i,k} + \mathbf{u}_{i,k}) < f(\mathbf{x}_{i,k})$, for $i = 1, ..., n_{pop}$, the population P_k converges to a single point in D for $k \to \infty$ with probability one.*

Proof: By contradiction let us assume that we do not have convergence to a fixed point. Then, it must hold

that:

$$\inf_k \max \left\{ \|\mathbf{x}_{i,k} - \mathbf{x}_{j,k}\|, i, j \in [1, ..., n_{pop}] \right\} \geq \epsilon > 0 \tag{14}$$

At every generation k the map can generate with a strictly positive probability, a displacement $F(\mathbf{x}_{i^*,k} - \mathbf{x}_{j^*,k})$ for $\mathbf{x}_{j^*,k}$, where i^* and j^* identify the individuals with the maximal reciprocal distance, such that the candidate point is $\mathbf{x}_{cand} = F\mathbf{x}_{i^*,k} + (1 - F)\mathbf{x}_{j^*,k}$ with $f(\mathbf{x}_{i^*,k}) \leq f(\mathbf{x}_{j^*,k})$. Since the function f is strictly quasi-convex, the candidate point is certainly better than $\mathbf{x}_{j^*,k}$ and, therefore, is accepted by S. Now, in view of Eq. (14) and of Lemma (II.2) we must have that,

$$f(\mathbf{x}_{cand}) \leq f(\mathbf{x}_{j,k}) - \delta_r(\epsilon) \tag{15}$$

Such reduction will occur with probability one infinitely often, and consequently the function value of at least one individual will be, with probability one, infinitely often reduced by $\delta_r(\epsilon)$. But in this way the value of the objective function of such individual would diverge to $-\infty$, which is a contradiction because f is bounded from below over the compact set D. ∎

If a local minimum satisfies some regularity assumptions (e.g., the Hessian at the local minimum is definite positive), then we can always define a neighborhood such that: (i) map (7) will be unable to accept points outside the neighborhood; (ii) the function is strictly convex within the neighborhood. Therefore, if at some iteration k the population P_k belongs to such a neighborhood, we can guarantee that map (10) will certainly converge to a fixed point made up by n_{pop} replications of a single point belonging to the neighborhood. For general functions, we can not always guarantee that the population will converge to a fixed point, but we can show that the maximum difference between the objective function values in the population converges to 0, i.e. the points in the population tend to belong to the same level set. The proof is closely related to that of Theorem II.1 and we still need to assume that indices i_1 and i_2 can be equal.

THEOREM II.4 *Assume that index i_1 can be equal to i_2. Given a function f, limited from below over D, and a population $P_k \in D$, then if $F \in (0, 1)$ and $S(\mathbf{x}_{i,k} + \mathbf{u}_{i,k}, \mathbf{x}_{i,k}) = 1 \Leftrightarrow f(\mathbf{x}_{i,k} + \mathbf{u}_{i,k}) < f(\mathbf{x}_{i,k})$, for $i = 1, ..., n_{pop}$, the following holds*

$$\max_{i,j \in [1,...,n_{pop}]} | f(\mathbf{x}_{j,k}) - f(\mathbf{x}_{i,k}) | \rightarrow 0, \tag{16}$$

as $k \rightarrow \infty$ with probability one.

Proof: Let S_k^* denote the set of best points in population P_k, i.e.

$$S_k^* = \left\{ \mathbf{x}_{j,k} \; : \; f(\mathbf{x}_{j,k}) \leq f(\mathbf{x}_{i,k}) \;\; \forall \, i \in [1, \ldots, n_{pop}] \right\} \tag{17}$$

At each iteration k there is a strictly positive probability that the whole population will be reduced to S_k^* at the next iteration. To show this it is enough to substitute the condition stated in (11) with the following condition

$$i_3 \in \left\{ i \; : \; x_{i,k} \in S_k^* \right\}$$

(basically, with respect to Theorem II.1, we only drop the requirement that at each iteration the best value of the population is attained at a single point).

In other words, there is a strictly positive probability for the event that the population at a given iteration will be made up of points all with the same objective function value. Therefore, such an event will occur infinitely often with probability one. Let us denote with $\{k_h\}_{h=1,\ldots}$ the infinite subsequence of iterations at which the event is true, and let

$$\Delta_h = f(\mathbf{x}_{i,k_h}) - f(\mathbf{x}_{i,k_{h+1}}) \tag{18}$$

be the difference in the objective function values at two consecutive iterations k_h and k_{h+1} (note that, since at iterations k_h, $h = 1,\ldots$ the objective function values are all equal and any i can be employed in the above definition). It holds that for all $i, j \in [1, \ldots, n_{pop}]$

$$\mid f(\mathbf{x}_{j,k}) - f(\mathbf{x}_{i,k}) \mid \leq \Delta_h \quad \forall \ k \in [k_h, k_{h+1}] \tag{19}$$

Therefore, if we are able to prove that $\Delta_h \to 0$, as $h \to \infty$, then we can also prove the result of our theorem. Let us assume by contradiction that $\Delta_h \not\to 0$. Then, there will exist a $\delta > 0$ such that $\Delta_h \geq \delta$ infinitely many times. But this would lead to function values diverging to $-\infty$ and, consequently, to a contradiction. ∎

As a consequence of these results, for the choice of the index i_1, i_2 and i_3 non-mutually different, a possible stopping criterion for the dynamics in Eq. (7) would be to stop when the difference between the function values in the population drops below a given threshold. However, this could cause a premature halt of the evolutionary process. Indeed, even if at some iteration the function value at all points of the population is equal, this does not necessarily mean that the algorithm will be unable to make further progress (unless all points in the population are multiple copies of a unique point). Therefore, since the evolution definitely ceases when the population contracts to a single point, we can alternatively use as a stopping criterion the fact that the maximum distance between points in the population drops below a given threshold.

It is important to observe that the contraction of the population does not depend on whether the function f is minimized or maximized but depends only on the definition of S and on whether the function is bounded or unbounded.

To further verify the contraction properties of the dynamics in Eq. (7) one can look at the eigenvalues of the matrix $\mathbf{J}_k$.

If the population cannot diverge, the eigenvalues cannot have a norm always > 1. Furthermore, according to Theorem II.3 if the function f is strictly quasi-convex in D, the population converges to a single point in D, which implies that the map (7) is a contraction in D and therefore the eigenvalues should have a norm on average lower than 1. This can be illustrated with the following test: Consider a population of 8 individuals and a D enclosing the minimum of a paraboloid with the minimum at the origin. For a C_R=1.0 and F=0.8, we compute, for each step k, the distances of the closest and farthest individuals from the local minimum and the eigenvalues of the matrix $\mathbf{J}$. Fig. 1 shows the behavior of the eigenvalues and of the distance from the origin. From the figure, we can see that for all iterations, the value of the norm of all the eigenvalues is in the interval $[0, 1]$ except for one eigenvalue
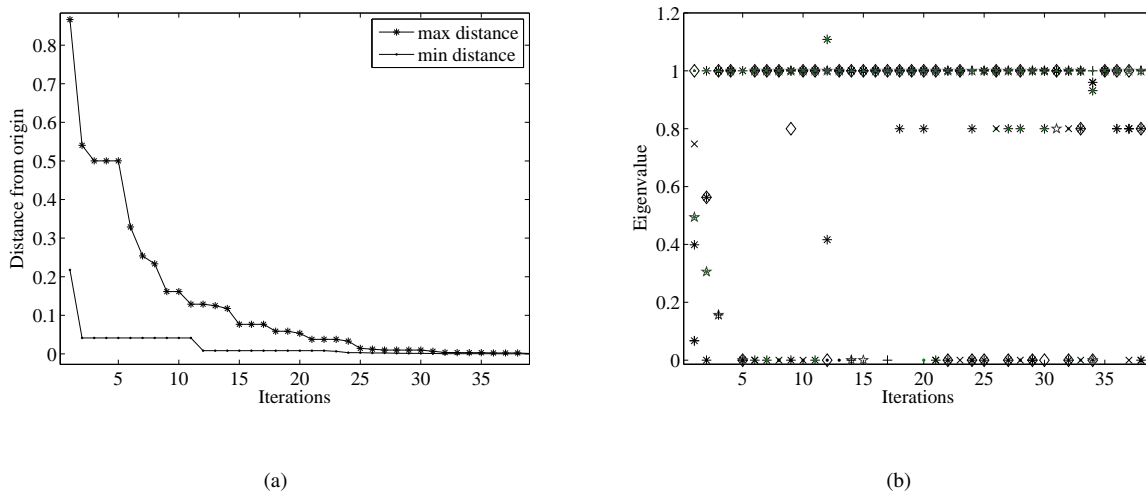
Fig. 1.   Contraction of map (10): a) max and min distance of the individuals in the population from the origin, b) eigenvalues with the number of evolutionary iterations.

at iteration 12. However, since every expansion is not accepted by the selection function S and for each iteration a number of eigenvalues have modulus lower than 1, the population contracts as represented in Fig. 1(a).

If multiple minima are contained in D, then it can be experimentally verified that the population contracts to a number of clusters initially converging to a number of local minima and eventually to the lowest among all the identified local minima.

The local convergence properties of map (7) suggest its hybridization with the heuristic implemented in Monotonic Basin Hopping (MBH).

MBH, first introduced in [14] in the context of molecular conformation problems) is a simple but effective global optimization method. At each iteration MBH: (i) generates a sample point within a neighborhood of size 2Δ of the current local minimum (e.g., by a random displacement of each coordinate of the current local minimum); (ii) starts a local search from the newly generated sample point; (iii) moves to the newly detected local minimum only if its function value is better than the function value at the current local minimum. The initial local minimum is usually randomly generated within the feasible region. Moreover, if no improvement is observed for a predetermined number of sample points $n_{samples}$, a restart mechanism might be activated. The neighborhood of the local minimum $\mathbf{x}_l$ is defined as $[\mathbf{x}_l - \Delta, \mathbf{x}_l + \Delta]^d$. A proper definition of Δ is essential for the performance of MBH: too small a size would not allow MBH to escape from the current local minimum, while too large a value would make the search degenerate in a completely random one. The local search performed at each iteration can be viewed as a *dynamical system* where the evolution of the systems at each iteration is controlled by some *map*. Under suitable assumptions, the systems converge to a fixed point. For instance, if f is convex and C^2 in a small enough domain containing a local minimum which satisfies some regularity conditions, Newton's map converges quadratically to a single fixed

point (the local minimum) within the domain. This observation leads to the above mentioned hybridization of DE with MBH: the dynamical system corresponding to a local search is replaced by the one corresponding to DE. More precisely, if map (7), either for a cluster $P_{sub} \subseteq P_k$ or for the entire population P_k, contracts, we can define a bubble $D_l \subseteq D$, around the best point within the cluster $\mathbf{x}_{best}$, and re-initialize a subpopulation P_{sub} in D_l. Such operation is performed as soon as the maximum distance $\rho_A = \max(\|\mathbf{x}_i - \mathbf{x}_j\|)$ among the elements in the cluster collapses below a value $tol_{conv}\rho_{A,max}$, where $\rho_{A,max}$ is the maximum ρ_A recorded during the convergence of the map (10).

In order to speed up convergence, the best solution $\mathbf{x}_{best}$ of the cluster is refined through a local search started at it, leading to a local minimum $\mathbf{x}_l$, which is saved in an archive A_g. The bubble is defined, similarly to the neighborhood of MBH, as $D_l = [\mathbf{x}_l - \Delta \ \mathbf{x}_l + \Delta]^d$. The overall process leads to Algorithm 1. Note that the contraction of the population given, for example, by the metric ρ_A, is a stopping criterion that does not depend explicitly on the value of the objective function but on the contractive properties of the map in Eq. (7). Some remarks follow.

1. Convergence of DE to a single point can not always be guaranteed, and consequently, we can not always guarantee that the contraction condition $\rho_A \leq tol_{conv}\rho_{A,max}$ will be satisfied at some iteration. Therefore, in order to take into account this possibility, we need to introduce a further stopping criterion for DE, such as a maximum number of iterations. We point out, however, that such alternative stopping criterion has never become active in our experiments.

2. Even when DE converges to a single point, this is not guaranteed to be a local minimum. For this reason we always refine the best observed solution through a local search.

3. If the search space is characterized by a single funnel structure [15], the restart of the population in the bubble allows the algorithm to move towards the global optimum by progressively jumping from one minimum to a better one. On the other hand, if multiple funnels or multiple isolated minima exist, a simple restart of the population inside a bubble might not be sufficient to avoid stagnation. A way to overcome this problem is to use global re-sampling: when the value of the best solution does not change for a predefined number of iterations iun_{max}, the population is restarted. The restart procedure collects the solutions in the archive into n_c clusters with baricenter $x_{c,j}$ for $j = 1, ..., n_c$, then each agent $\mathbf{x}_i$ of the new population is generated so that $\|\mathbf{x}_i - \mathbf{x}_{c,j}\| > \delta_c$. Note that a restart mechanism for DE was previously proposed also by Peng et al. [16] in a variant of the adaptive Differential Evolution JADE. However, in the work of Peng et al. the restart criterion and restart strategy are substantially different from the ones proposed here. For example, although we record the local minima in an external archive, we do not prevent the algorithm from searching in the surroundings of the recorded minima. On the contrary, we combine a local restart in a bubble surrounding the final point returned by DE, according to the heuristics of MBH, with a more global restart sampling outside the bubbles. A complete review of the existing variants of Differential Evolution can found in the work of Neri et al. [17]. Other restart mechanisms have recently been adopted to improve other evolutionary algorithms such as G-CMAES [18] or hybrid methods [19], but also in these cases the restart criterion and restart strategy are

substantially different from the ones proposed here.

4. A question, mainly of theoretical interest, is about convergence. General results stating conditions under which convergence to the global minimum (with probability 1) is guaranteed can be found, e.g., in [20] and [21]. Such conditions are not fulfilled by standard DE, while IDEA fulfills them if parameter δ_c employed in the restart mechanism is "small enough" (if too large, some portions of the feasible region, possibly including the global minimum, might remain unexplored). We point out that, although in practice we are not interested in the behavior of an algorithm over an infinite time horizon, global convergence justifies re-running the search process with an increased number of function evaluations should the results be unsatisfactory. As we will show in the remainder of this paper, IDEA produces performance steadily increasing with the number of function evaluations without the need to change its settings.

III. TRAJECTORY MODEL AND PROBLEM FORMULATION

The modified differential evolution algorithm derived in Section II is applied to the solution of four real world cases. The four cases are all multigravity assist (MGA) trajectory design problems, three of them with deep space manoeuvres (DSM) and one with no DSM's. In this section we describe the trajectory model and we formulate the global optimization problem that will be tackled through Algorithm 1.

A. Trajectory Model with no DSM's

Multi-gravity assist transfers with no deep space maneuvers can be modeled with a sequence of conic arcs connecting a number of planets. The first one is the departure planet, the last one is the destination planet and at all the intermediate ones the spacecraft performs a gravity assist maneuver. Given N_P planets P_i with $i = 1, ..., N_P - 1$, each conic arc is computed as the solution of a Lambert's problem [22] given the departure time from planet P_i and the arrival time at planet P_{i+1}. The solution of the Lambert's problems yields the required incoming and outgoing velocities at a swing-by planet v_{in} and v_{rout} (see Fig. 2). The swing-by is modeled through a linked-conic approximation with powered maneuvers [23], i.e., the mismatch between the required outgoing velocity v_{rout} and the achievable outgoing velocity v_{aout} is compensated through a Δv maneuver at the pericenter of the gravity assist hyperbola. The whole trajectory is completely defined by the departure time t_0 and the transfer time for each leg T_i, with $i = 1, ..., N_P - 1$.

The normalized radius of the pericenter $r_{p,i}$ of each swing-by hyperbola is derived a posteriori once each powered swing-by manoeuvre is computed. Thus, a constraint on each pericenter radius has to be introduced during the search for an optimal solution. In order to take into account this constraint, the objective function is augmented with the weighted violation of the constraints:

$$f(\mathbf{x}) = \Delta v_0 + \sum_{i=1}^{N_p-2} \Delta v_i + \Delta v_f + \sum_{i=1}^{N_p-2} w_i(r_{p,i} - r_{pmin,i})^2 \qquad (20)$$

for a solution vector:

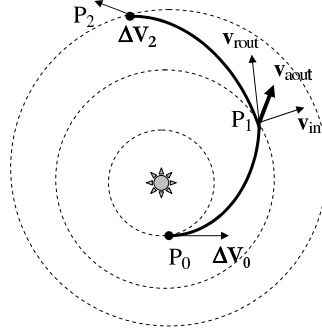$$\mathbf{x} = [t_0, T_1, T_2, ..., T_{N_P-1}]^T \qquad (21)$$

Fig. 2.   Trajectory model with no DSM's

B. Trajectory Model with DSM's

A general MGA-DSM trajectory can be modeled through a sequence of $N_P - 1$ legs connecting N_P celestial bodies (Fig. 3) [24]. In particular if all celestial bodies are planets, each leg begins and ends with an encounter with a planet. Each leg i is made of two conic arcs: the first, propagated analytically forward in time, ends where the second solution of a Lambert's problem begins. The two arcs have a discontinuity in the absolute heliocentric velocity at their matching point M. Each DSM is computed as the vector difference between the velocities along the two conic arcs at the matching point. Given the transfer time T_i and the variable $\alpha_i \in [0, 1]$ relative to each leg i, the matching point is at time $t_{DSM,i} = t_{f,i-1} + \alpha_i T_i$, where $t_{f,i-1}$ is the final time of the leg $i - 1$. The relative velocity vector $\mathbf{v}_0$ at the departure planet can be a design parameter and is expressed as:

$$\mathbf{v}_0 = v_0[\sin\delta\cos\theta, \sin\delta\sin\theta, \cos\delta]^T \tag{22}$$

with the angles δ and θ respectively representing the declination and the right ascension with respect to a local reference frame with the x axis aligned with the velocity vector of the planet, the z axis normal to orbital plane of the planet and the y axis completing the coordinate frame. This choice allows for an easy constraint on the escape velocity and asymptote direction while adding the possibility of having a deep space maneuver in the first arc after the launch. This is often the case when the escape velocity must be fixed due to the launcher capability or to the requirement of a resonant swing-by of the Earth (Earth-Earth transfers). In order to have a uniform distribution of random points on the surface of the sphere defining all the possible launch directions, the following transformation has been applied:

$$\bar{\theta} = \frac{\theta}{2\pi} \qquad \bar{\delta} = \frac{\cos(\delta + \pi/2) + 1}{2} \tag{23}$$

It results that the sphere surface is uniformly sampled when a uniform distribution of points for $\bar{\theta}, \bar{\delta} \in [0, 1]$ is chosen. Once the heliocentric velocity at the beginning of leg i, which can be the result of a swing-by maneuver or the asymptotic velocity after launch, is computed, the trajectory is analytically propagated until time $t_{DSM,i}$. The second arc of leg i is then solved through a Lambert's algorithm, from M_i, the Cartesian position of the deep space maneuver, to P_i, the position of the target planet of phase i, for a time of flight $(1 - \alpha_i)T_i$. Two subsequent legs
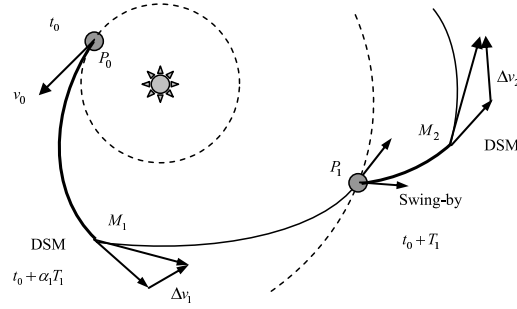
Fig. 3. Schematic representation of a multiple gravity assist trajectory
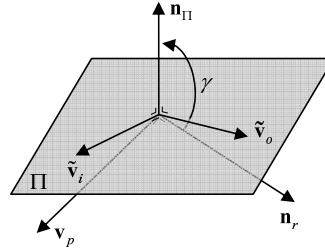

Fig. 4. Schematic representation of a multiple gravity assist trajectory

are then joined together with a gravity assist manoeuvre. The effect of the gravity of a planet is to instantaneously change the velocity vector of the spacecraft.

The relative incoming velocity vector and the outgoing velocity vector at the planet swing-by have the same modulus but different directions; therefore the heliocentric outgoing velocity results to be different from the heliocentric incoming one. In the linked conic model, the spacecraft is assumed to follow a hyperbolic trajectory with respect to the swing-by planet. The angular difference between the incoming relative velocity $\tilde{\mathbf{v}}_i$ and the outgoing one $\tilde{\mathbf{v}}_o$ depends on the modulus of the incoming velocity and on the pericenter radius r_i. Both the relative incoming and outgoing velocities belong to the plane of the hyperbola. However, in the linked-conic approximation, the maneuver is assumed to occur at the planet, where the planet is a point mass coinciding with its center of mass. Therefore, given the incoming velocity vector, one angle is required to define the attitude of the plane of the hyperbola Π. Although there are different possible choices for the attitude angle γ, the one proposed in Ref. 7 has been adopted (see Fig. 4), where γ is the angle between the vector $\mathbf{n}_\Pi$, normal to the hyperbola plane Π, and the reference vector $\mathbf{n}_r$, normal to the plane containing the incoming relative velocity and the velocity of the planet $\mathbf{v}_P$.

Given the number of legs of the trajectory $N_L = N_P - 1$, the complete solution vector for this model is:

$$\mathbf{x} = [v_0, \bar{\theta}, \bar{\delta}, t_0, \alpha_1, T_1, \gamma_1, r_{p,1}, \alpha_2, T_2, ..., \tag{24}$$

$$\gamma_i, r_{p,i}, T_{i-1}, \alpha_{i-1}, ..., \gamma_{N_L-1}, r_{p,N_L-1}, \alpha_{N_L}, T_{N_L}]$$

where t_0 is the departure date. Now, the design of a multi-gravity assist transfer can be transcribed into a general

nonlinear programming problem, with simple box constraints, of the form:

$$\min_{\mathbf{x} \in D} f(\mathbf{x}) \tag{25}$$

One of the appealing aspects of this formulation is its solvability through a general global search method for box constrained problems. Depending on the kind of problem under study, the objective function can be defined in different ways. Here we choose to focus on minimizing the total Δv of the mission, therefore the objective function $f(\mathbf{x})$ is:

$$f(\mathbf{x}) = v_0 + \sum_{i=1}^{N_p} \Delta v_i + \Delta v_f \tag{26}$$

where Δv_i is the velocity change due to the DSM in the i-th leg, and Δv_f is the maneuver needed to inject the spacecraft into the final orbit.

IV. TEST PROBLEMS

We consider a benchmark made of four different test-cases: two versions of the MGA transfer from the Earth to Saturn of the Cassini-Huygens mission, a multi-gravity assist transfer to the comet 67P/Churyumov-Gerasimenko (similar to the Rosetta mission), and a multi-gravity assist rendezvous transfer with mid-course manoeuvres to Mercury (similar to the Messenger mission). Algorithm 1, called IDEA, is applied to the solution of the four cases and compared to standard Differential Evolution [5] and Monotonic Basin Hopping [14], [25].

A. Cassini with no DSM's

The first test case is a multi gravity assist trajectory from the Earth to Saturn following the sequence Earth-Venus-Venus-Earth-Jupiter-Saturn (EVVEJS). There are six planets and the transfer is modeled as in Section III-A, thus the solution vector is:

$$\mathbf{x} = [t_0, T_1, T_2, T_3, T_4, T_5]^T \tag{27}$$

The final Δv_f is the Δv needed to inject the spacecraft into an ideal operative orbit around Saturn with a pericenter radius of 108950 km and an eccentricity of 0.98. The weighting functions w_i are defined as follows:

$$w_i = 0.005[1 - \text{sign}(r_{p,i} - r_{pmin,i})], \quad i = 1, ..., 3 \tag{28}$$

$$w_4 = 0.0005[1 - \text{sign}(r_{p,4} - r_{pmin,4})]$$

with the minimum normalized pericenter radii $r_{pmin,1} = 1.0496$, $r_{pmin,2} = 1.0496$, $r_{pmin,3} = 1.0627$ and $r_{pmin,4} = 9.3925$. For this case the dimensionality of the problem is six, with the search space D defined by the following intervals: $t_0 \in [-1000, 0]$MJD2000, $T_1 \in [30, 400]$d, $T_2 \in [100, 470]$d, $T_3 \in [30, 400]$d, $T_4 \in [400, 2000]$d, $T_5 \in [1000, 6000]$d. The best known solution is $f_{best} = 4.9312$ km/s, with $\mathbf{x}_{best}$=[–789.75443770458, 158.301628961437, 449.385882183958, 54.7050296906556, 1024.5997453164, 4552.72068790619]^T.

B. Cassini with DSM's

The second test case is again a multi gravity assist trajectory from the Earth to Saturn following the sequence Earth-Venus-Venus-Earth-Jupiter-Saturn (EVVEJS), but a deep space manoeuvre is allowed along the transfer arc from one planet to the other according to the model presented in Section III-B. Although from a trajectory design point of view, this problem is similar to the first test case, the model is substantially different and therefore represents a different problem from a global optimization point of view. Since the transcription of the same problem into different mathematical models can affect the search for the global optimum, it is interesting to analyze the behavior of the same set of global optimization algorithms applied to two different transcriptions of the same trajectory design problem.

Here, Δv_f is defined as the modulus of the vector difference between the velocity of Saturn at arrival and the velocity of the spacecraft at the same time. For this case the dimensionality of the problem is 22, with the search space D is defined by the following intervals: $t_0 \in [-1000, 0]$MJD2000, $v_0 \in [3, 5]$km/s, $\bar{\theta} \in [0, 1]$, $\bar{\delta} \in [0, 1]$, $T_1 \in [100, 400]$d, $T_2 \in [100, 500]$d, $T_3 \in [30, 300]$d, $T_4 \in [400, 1600]$d, $T_5 \in [800, 2200]$d, $\alpha_1 \in [0.01, 0.9]$, $\alpha_2 \in [0.01, 0.9]$, $\alpha_3 \in [0.01, 0.9]$, $\alpha_4 \in [0.01, 0.9]$, $\alpha_5 \in [0.01, 0.9]$, $r_{p,1} \in [1.05, 6]$, $r_{p,2} \in [1.05, 6]$, $r_{p,3} \in [1.15, 6.5]$, $r_{p,4} \in [1.7, 291]$, $\gamma_1 \in [0, 2\pi]$, $\gamma_2 \in [0, 2\pi]$, $\gamma_3 \in [0, 2\pi]$, $\gamma_4 \in [0, 2\pi]$. The best known solution is $f_{best} = 8.3889$ km/s, $\mathbf{x}_{best}$=[–780.917853635368, 3.27536879103551, 0.782513100225235, 0.378682006044345, 169.131920055057, 424.13242396494, 53.296452710059, 2199.98648654574, 0.795774035295027, 0.530055267286, 0.126002760289258, 0.0105947672634, 0.0381505843013, 1.35556902792788, 1.05001740672886, 1.30699201995999, 71.3749247783128, 3.15842153037544, 3.53046280721895, 3.12561791754698, 3.08422162979462]^T.

C. Rosetta Mission

The third test case is a multi gravity assist trajectory from the Earth to the comet 67P/Churyumov-Gerasimenko following the gravity assist sequence that was planned for the spacecraft Rosetta: Earth-Earth-Mars-Earth-Earth-Comet. The trajectory model is the one described in Section III-B but the objective function does not include v_0.

For this case the dimensionality of the problem is 22, with the search space D is defined by the following intervals: $t_0 \in [1460, 1825]$MJD2000, $v_0 \in [3, 5]$km/s, $\bar{\theta} \in [0, 1]$, $\bar{\delta} \in [0, 1]$, $T_1 \in [300, 500]$d, $T_2 \in [150, 800]$d, $T_3 \in [150, 800]$d, $T_4 \in [300, 800]$d, $T_5 \in [700, 1850]$d, $\alpha_1 \in [0.01, 0.9]$, $\alpha_2 \in [0.01, 0.9]$, $\alpha_3 \in [0.01, 0.9]$, $\alpha_4 \in [0.01, 0.9]$, $\alpha_5 \in [0.01, 0.9]$, $r_{p,1} \in [1.05, 9]$, $r_{p,2} \in [1.05, 9]$, $r_{p,3} \in [1.05, 9]$, $r_{p,4} \in [1.05, 9]$, $\gamma_1 \in [0, 2\pi]$, $\gamma_2 \in [-\pi, \pi]$, $\gamma_3 \in [0, 2\pi]$, $\gamma_4 \in [0, 2\pi]$.

The best known solution is f_{best}=1.34229 km/s, with solution vector x_{best}=[1542.65536672006, 4.48068107888312, 0.935220667497966, 0.9909562486258, 365.24235847396, 707.540858648698, 257.417859715383, 730.483434305258, 1850, 0.310501108489873, 0.809061227121068, 0.0124756484551758, 0.0466967002704, 0.43701236871638, 1.8286351998512, 1.05, 2.80973511169638, 1.18798981835459, 2.61660601734377, –0.215250274241349, 3.57950314115394, 3.46467471264343]^T.

D. Messenger Mission

The fourth problem is a multi-gravity assist trajectory from the Earth to planet Mercury following the sequence of planetary encounters of the first part of the Messenger mission. As for the previous test case, the trajectory model is the one described in Section III-B.

For this case the dimensionality of the problem is 18, with the search space D is defined by the following intervals: $t_0 \in [1000, 4000]$MJD2000, $v_0 \in [1, 5]$km/s, $\bar{\theta} \in [0, 1]$, $\bar{\delta} \in [0, 1]$, $T_1 \in [200, 400]$d, $T_2 \in [30, 400]$d, $T_3 \in [30, 400]$d, $T_4 \in [30, 400]$d, $\alpha_1 \in [0.01, 0.99]$, $\alpha_2 \in [0.01, 0.99]$, $\alpha_3 \in [0.01, 0.99]$, $\alpha_4 \in [0.01, 0.99]$, $r_{p,1} \in [1.1, 6]$, $r_{p,2} \in [1.1, 6]$, $r_{p,3} \in [1.1, 6]$, $\gamma_1 \in [-\pi, \pi]$, $\gamma_2 \in [-\pi, \pi]$, $\gamma_3 \in [-\pi, \pi]$.

The best known solution is f_{best} = 8.631 km/s, with solution vector $\mathbf{x}_{best}$=[1171.14619813253, 1.41951376601752, 0.628043728560056, 0.500000255697689, 399.999999999969, 178.921469111868, 299.279691870106, 180.689114497891, 0.236414009949924, 0.0674215615945254, 0.832992171208578, 0.312514378885353, 1.7435422021558, 3.03087330660319, 1.10000000000119, 0.219820823285448, 0.477475660779879, 0.225898117795826]^T.

Note that, the search space for each one of the trajectory models is normalized so that D is a unit hypercube with each component of the solution vector belonging to the interval $[0, 1]$. Furthermore, for all cases, solution algorithms were run for a progressively increasing number of function evaluations from 100000 to 1.25 million.

V. TESTING PROCEDURE

The modified DE algorithm will be compared against standard DE and MBH following a rigorous testing procedure. A detailed description of the testing procedure can be found in [26] and it is here summarized in Algorithm 2 for a generic solution algorithm A and a generic problem p. Here $\bar{\mathbf{x}}(A, i)$ denotes the best point observed during the i-th run of algorithm A.

The index of performance j_s is the number of successes of the algorithm A. In the following we use the f_{best} values reported above in place of f_{global} and we consider only $\delta_f(\bar{\mathbf{x}}(A, i))$ and not $\delta_x(\bar{\mathbf{x}}(A, i))$.

The success rate, $p_s = j_s/n$, will be used for the comparative assessment of the algorithm performance instead of the commonly used best value, mean and variance. Indeed, the distribution of the function values is not Gaussian. Therefore, the average value can be far away from the results returned with a higher frequency from a given algorithm. In the same way, the variance is not a good indicator of the quality of the algorithm because a high variance together with a high mean value can correspond to the case in which 50% of the results are close to the global optimum with the other 50% far from it. Finally, statistical tests, such as the t-test, that assume a Gaussian distribution of the sample can not be applied to correctly predict the behavior of an algorithm. Instead, the success rate gives an immediate and unique indication of the algorithm effectiveness, and, moreover, it can be always represented with a binomial probability density function (pdf), independent of the number of function evaluations, the problem and the type of optimization algorithm.

A key point is setting properly the value of n to have a reliable estimate of the success probability of an algorithm, or success rate $p_s = j_s/n$. Since the success is binomial (assumes values that are either 0 or 1) we can set a priori

the value of n to get the required confidence on the value of p_s. A commonly adopted starting point for sizing the sample of a binomial distribution is to assume a normal approximation for the sample proportion p_s of successes (i.e. $p_s \sim N\{\theta_p, \theta_p(1 - \theta_p)/n\}$, where θ_p is the unknown true proportion of successes) and the requirement that $Pr[|p_s - \theta_p| \leq d_{err}|\theta_p]$ is at least equal to $1 - \alpha_p$ [27]. This leads to the expression $n \geq \theta_p(1 - \theta_p)\chi^2_{(1),\alpha_p}/d^2_{err}$ that can be approximated conservatively with

$$n \geq 0.25\chi^2_{(1),\alpha_p}/d^2_{err} \tag{29}$$

valid for $\theta_p = 0.5$. According to Eq. (29), an error ≤ 0.05 ($d_{err} = 0.05$) with a 95% of confidence ($\alpha_p = 0.05$) would require at least $n = 175$. If n is extended to 1000, the error reduces to 0.020857. In the following, we will use $n = 200$ and $N = 1.25e6$ for tuning the algorithms, and $n = 1000$ with variable N to compare their performance. In fact, a reduced error is required to discriminate between the performance of two algorithms at low N.

The values of tol_f for the four test cases are: $tol_f = 0.0688$ km/s for Cassini with no DSM's, $tol_f = 0.1111$ km/s for Cassini with DSM's, $tol_f = 0.05778$ km/s for Rosetta and $tol_f = 0.05$ km/s for Messenger. The choice of these thresholds was dictated by the need to discriminate among different minima. At the same time they represent a reasonable margin on the total Δv. In fact, during standard preliminary designs, a margin between 3% and 5% is typically added for contingencies, while here all the selected thresholds are below 5% of the value of the objective function. In other words, all the minima within the thresholds would be indistinguishable from a mission design point of view.

A. Parameter Tuning

Prior to running the tests on all the four cases, the key parameters for DE and MBH were tuned to get the best performance. We used the Rosetta case as a tuning example. The tuning of DE and MBH is used also to tune IDEA. The tuning of MBH was relatively fast as there are only two parameters: the size of the neighborhood and the number of samples before global restart.

Figure 5 shows the performance of MBH on the Rosetta case for different values of Δ and $n_{samples}$. It can be noted that the performance tends to increase for a number of samples that tend to infinity. On the other hand, there is a peak of performance around $n_{samples} = 30$. In the remainder of this paper, we will call MBH-GR the version of MBH implementing a global restart after 30 unsuccessful samples and we call MBH, the version with $n_{samples} = \infty$. The optimum Δ seems to be 0.1, therefore this value was used for all the test cases.

Note that the general trend of the performance of MBH does not change for the other cases and therefore the settings seem to be of general validity for this benchmark of test problems.

For the tuning of DE, we instead considered a grid of values for F, C_R and population size, for different strategies. Figs. 6 to 9 show the most significant results. From these figures one can deduce that strategy 6 with F in the range [0.8, 1] and a population below 200 individuals would be a good choice. Alternatively strategy 7 can be used with
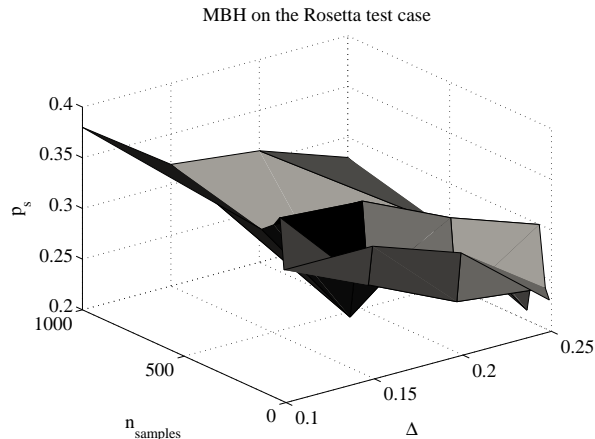
Fig. 5.   Performance of MBH on the Rosetta test case

a smaller population and an F in the range $[0.6, \ 0.7]$. In both cases C_R is better at around 0.8 as the problem is not separable and the components of the solution vector are interdependent.

The combination of strategy and values of F, n_{pop} controls the speed of local convergence to a fixed point of the algorithm. In the following tests, therefore, we decided to use strategy 6 with two sets of populations, $[5\,d, 10\,d]$, where d is the dimensionality of the problem, with single values of step-size and crossover probability $F = 0.75$ and $C_R = 0.8$ respectively. The two settings will be denoted with DE5, DE10. The trends in Figs. 6 to 9 can be registered also for the other two test cases, although the performance of DE is much poorer than for Rosetta, therefore it can be argued that the settings have general validity. These settings are also in line with the theory developed by Zaharie in [28].

The settings of IDEA were derived from the individual tuning of DE and MBH. In particular, we took a value $C_R = 0.9$, as the variables are not decoupled, a convergence strategy for the choice of the indexes in Eq. (4) and a value $F = 0.9$ together with a small population to have a fast convergence but without losing exploration capabilities. We used an $n_{pop} = 20$ for Cassini with no DSM's and for Messenger, while an $n_{pop} = 40$ for Rosetta and Cassini with DSM's. For all the test cases $\delta_c = 0.1$, $tol_{conv} = 0.25$, while $\Delta = 0.2$ for all the cases except for Messenger for which we used 0.25 instead. The parameter controlling the maximum number of local restarts is $iun_{max} = 6$ for Messenger, $iun_{max} = 2$ for Rosetta, $iun_{max} = +\infty$ for Cassini with and without DSM's as no guided restart is applied.

B. Test Results

The performance of all the algorithms are summarized in Figs. 10, 11, 12 and 13. For the Cassini case with no DSM's, with results shown in Fig. 10, IDEA performs exceptionally well compared to all the other algorithms providing a success rate over 50% at 200000 function evaluations. Both versions of DE exhaust their exploration capabilities quite soon and an increase of the number of function evaluations does not help as the population has

DE on the Rosetta test case. CR=0.8 Strategy=6
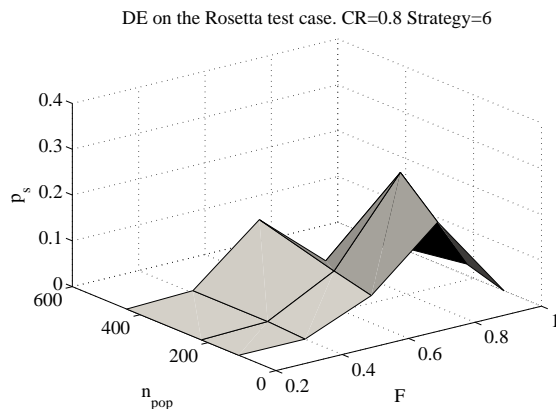
Fig. 6.   Performance of Differential Evolution on the Rosetta test case, with strategy 6 and CR=0.8

DE on the Rosetta test case. CR=0.8 Strategy=7
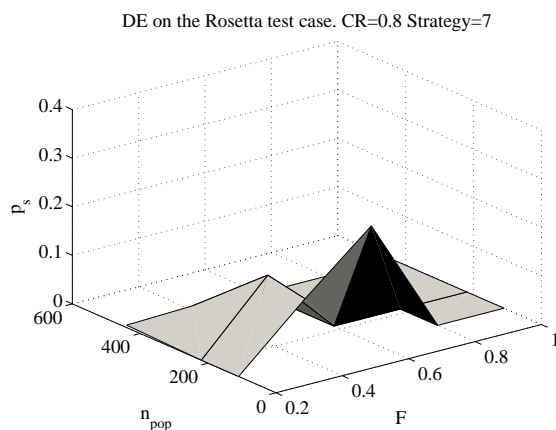
Fig. 7.   Performance of Differential Evolution on the Rosetta test case, with strategy 7 and CR=0.8

collapsed to a fixed point. The performance is not nearly as good on the Cassini case with DSM's, as seen in Fig. 11.

Although IDEA is still better than the other algorithms, and in particular than standard DE, it is comparable to MBH up to 600000 function evaluations and achieves a moderate 30% as best result at 1.25 million function evaluations. This poor performance seems to be due mainly to problems of local convergence. Note, however, how the general trend suggests that IDEA is not stagnating as the success rate is steadily increasing for an increasing number of function evaluations. On the contrary DE seems to reach a flat plateau. Even for the Rosetta case, IDEA displays exceptionally good results with DE5, DE10, MBH and MBH-GR substantially equivalent until $N \leq 800k$. After that, DE reaches a plateau and stops exploring. Both IDEA and MBH, instead, show a positive monotonic trend until $N = 1.25M$, but IDEA outperforms both versions of MBH.

In the Messenger case, all algorithms do not perform particularly well if $N \leq 500k$. Due to the structure of the problem, IDEA needs more time to converge under the tol_{conv} threshold and only after many re-sampling iterations is able to show good performance. On the other hand, all DE's do not display any significant improvement for
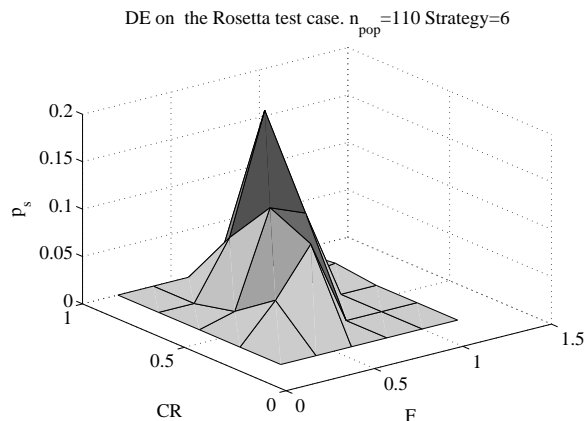
Fig. 8. Performance of Differential Evolution on the Rosetta test case, with strategy 6 and n_{pop}=110
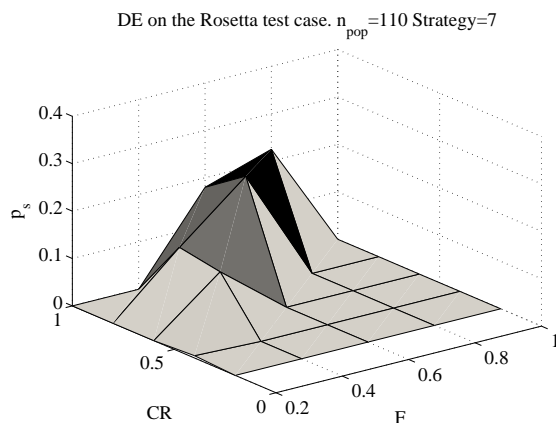
Fig. 9. Performance of Differential Evolution on the Rosetta test case, with strategy 7 and n_{pop}=110

more than $500k$ evaluations and even MBH can be considered equally ineffective (the difference between DE and MBH is lower then the confidence interval).

VI. SEARCH SPACE ANALYSIS

The different behaviors of IDEA, DE and MBH on the four test cases can be understood with an analysis of the structure of the search space. The collection of the results from the tests can be used to deduce some properties of the problems within the benchmark and to predict the behavior of the solution algorithms. An understanding of the characteristics of the benchmark is required to generalize the result of the tests. In fact, every consideration on the performance of the algorithms is applicable only to problems with similar characteristics.

All local minima found in all the tests by the applied global methods were grouped according to the value of their objective function. Specifically, the range of values of the objective function for each test was divided in a finite number of levels, with each group of minima associated to a particular level.
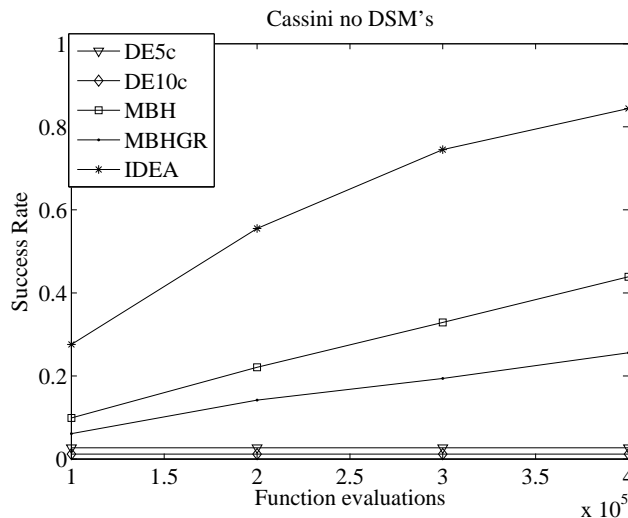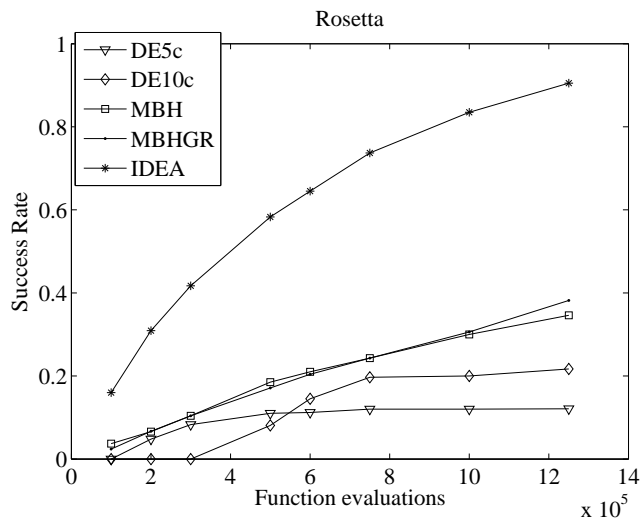
Fig. 10.   Variation of the success rate with the number of function evaluations, for the Cassini without DSM's test case
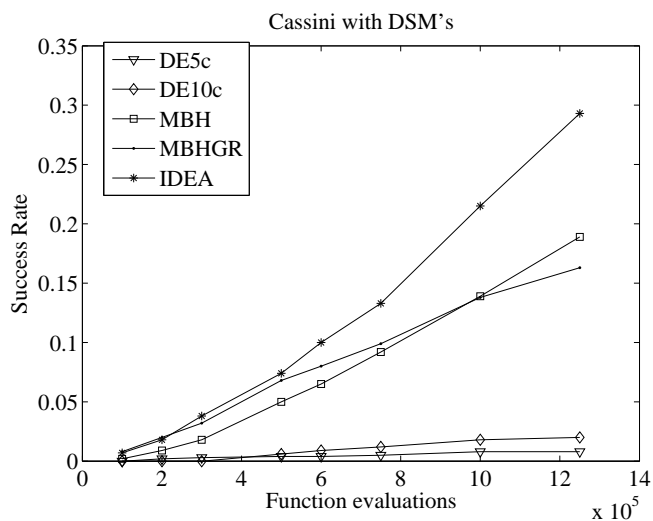
Fig. 11.   Variation of the success rate with the number of function evaluations, for the Cassini with DSM's test case

Then, we computed the average value of the relative distance of each local minimum with respect to all other local minima within the same level d_{il} (or intra-level distance), and the average value of the relative distance of each local minimum with respect to all other local minima in the lower level d_{tl} (or trans-level distance). The d_{tl} for the lowest level is the average distance with respect to the best known solution.

The values d_{il} and d_{tl} give an immediate representation of the diversity of the local minima and the probability of a transition from one level to another. More precisely, a cluster of minima with a large intra-level distance and a small trans-level distance suggests an easy transition to lower values of the objective function and a possible underlying funnel structure [12]. In particular in the case of funnel structures, the values of d_{tl} and d_{il} should progressively go to zero. A d_{il} that does not go to zero or clusters with different values of d_{tl}, are the cue to a possible underlying multi-funnel structure.

Fig. 12.   Variation of the success rate with the number of function evaluations, for the Rosetta test case
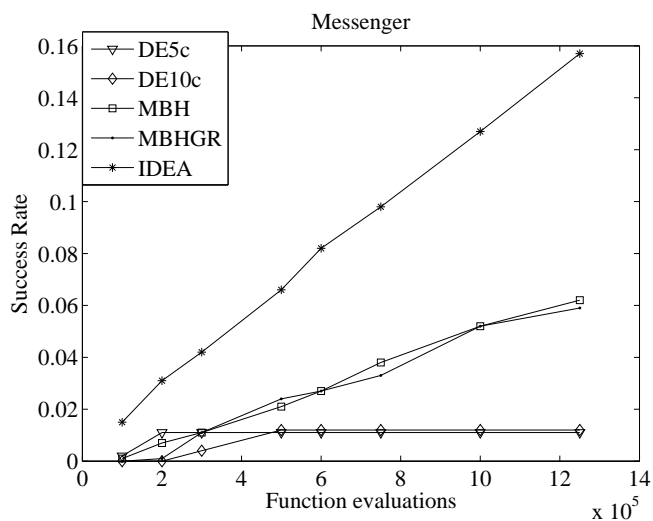
Fig. 13.   Variation of the success rate with the number of function evaluations, for the Messenger test case

Fig. 14 provide two illustrative examples. Fig. 14(a) represents a single funnel structure with five local minima $x_{l,i}$ where $i = 1, ..., 5$, and three levels. The intra-level distance at level 2, given by the distance $d_{24} = x_{l,2} - x_{l,4}$, is lower than $d_{15} = x_{l,1} - x_{l,5}$, the intra-level distance at level 1. The same is true for the trans-level distance at level 2, d_{23}, which is lower than the trans-level distance at level 1, $(d_{12} + d_{14})/2$, for minimum $x_{l,1}$.

Fig. 14(b), instead, represents a bi-funnel structure. In this case, the minima around $x_{l,6}$ have an average intra-level distance lower than $x_{l,2}$ but a trans-level distance d_{63} much larger than d_{23}. Thus, the two minima $x_{l,2}$ and $x_{l,6}$ will appear on the d_{tl}-d_{il} graph with different values of d_{il} and d_{tl}. If the threshold of level 3 were increased above the objective value of $x_{l,6}$, then all minima of level 2 would have similar d_{tl}, but the d_{il} at level 3 would not go to zero.

This analysis method is an extension of the work of Reeves and Yamada [9], and is used to concisely visualize
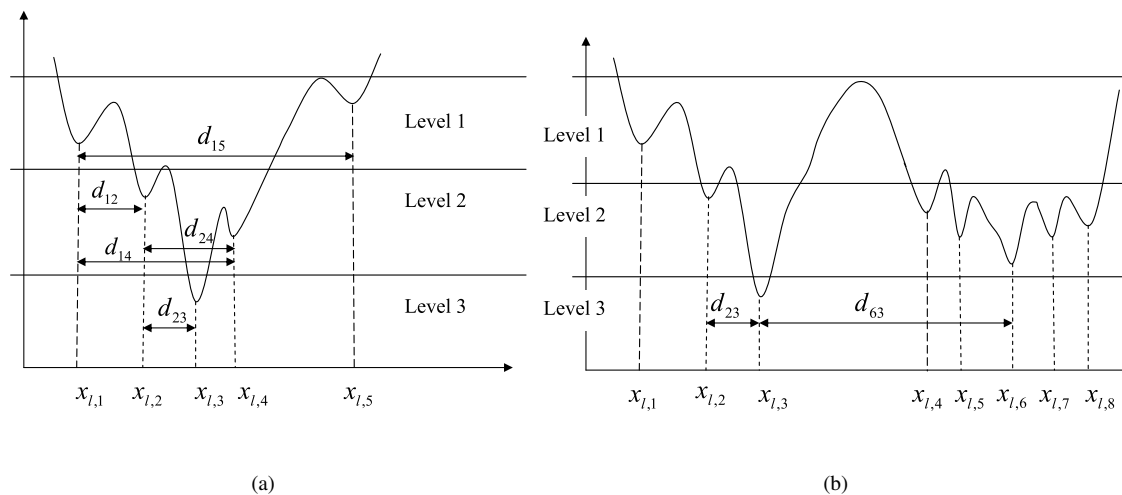
Fig. 14.   One dimensional example of a) single funnel structure and b) bi-funnel structure.
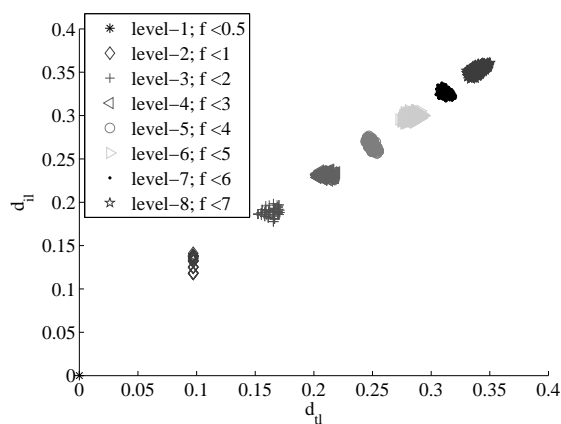
Fig. 15.   Relative distance of the local minima for the Rastrigin function in 5 dimensions

the distribution of the local minima. The definition of the levels depends on the groups of minima of interest, and can be derived from mission constraints or by an arbitrary subdivision of the range of values of the objective function. Different subdivisions reveal different characteristics of the search space but give only equivalent cues on the transition probability.

As an example of application of the proposed search space analysis method, Figs. 15 and 16 show the d_{il}-d_{tl} plots for two well known functions: Rastrigin and Schwefel. In both cases the dimensionality is 5. The Rastrigin function is known to have a single funnel and to be globally convex (see the example of one-dimensional Rastrigin function in Fig. 17(a)). The clusters in the d_{il}-d_{tl} plane are aligned along the diagonal and converge to 0. In the case of the Schwefel function, which has no single funnel structure (see the example of one-dimensional Schwefel function in Fig. 17(b)), the clusters are more scattered and both the d_{il} and d_{tl} values tend to remain quite high.
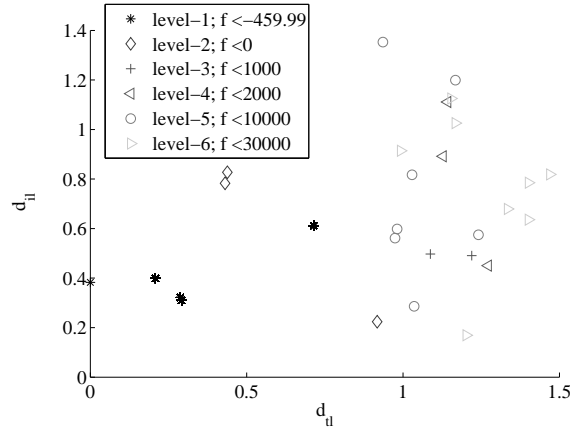
Fig. 16.   Relative distance of the local minima for the Schwefel function in 5 dimensions

(a)   (b)
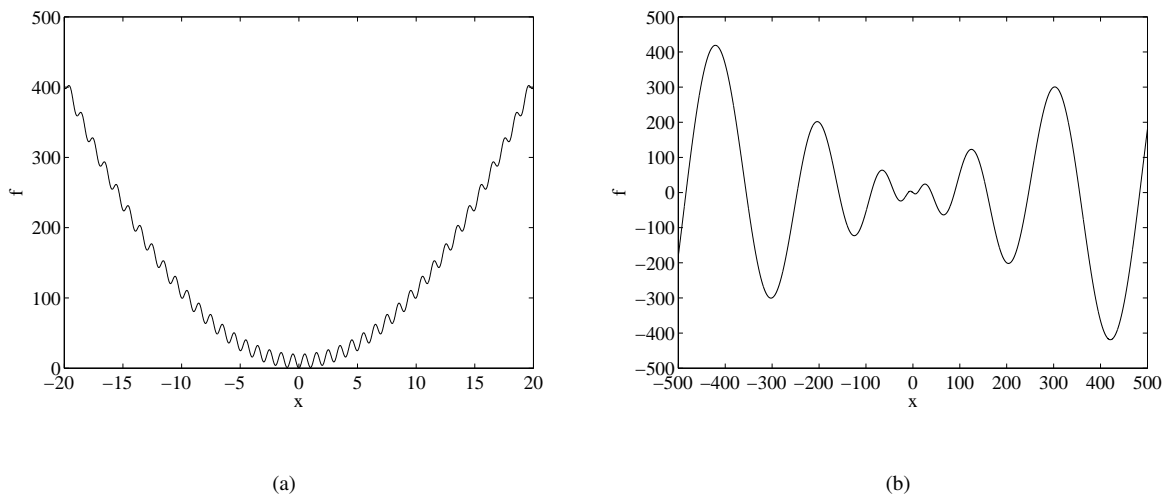
Fig. 17.   One dimensional example of a) Rastrigin function and b) Schwefel function.

When applied to the benchmark of space trajectory problems, the analysis approach seems to suggest (see Fig. 18(a)) that the Cassini case with no DSM's has a structure similar to the one in Fig. 14(b): the minima at level 5 belong to two distinct clusters with substantially different d_{tl} and d_{il}. The clusters, corresponding to levels 1, 2 and 3, have values of d_{tl} and d_{il} both lower than 0.2, which suggests an easy transition from one level to an another. Thus, below an objective function of 7.5 km/s there seems to be an underlying single funnel structure. Note that an easy transition among levels favors the search mechanism of MBH as demonstrated by the test results.

Fig. 18(b) shows that both d_{tl} and d_{il} progressively tend to zero up to a certain point, after which d_{tl} goes to zero while d_{il} remains almost unchanged. The figure suggests that, in the Cassini case with DSM, there is a single funnel structure for function values above 9.5 km/s, while below the minima are scattered and distant from each
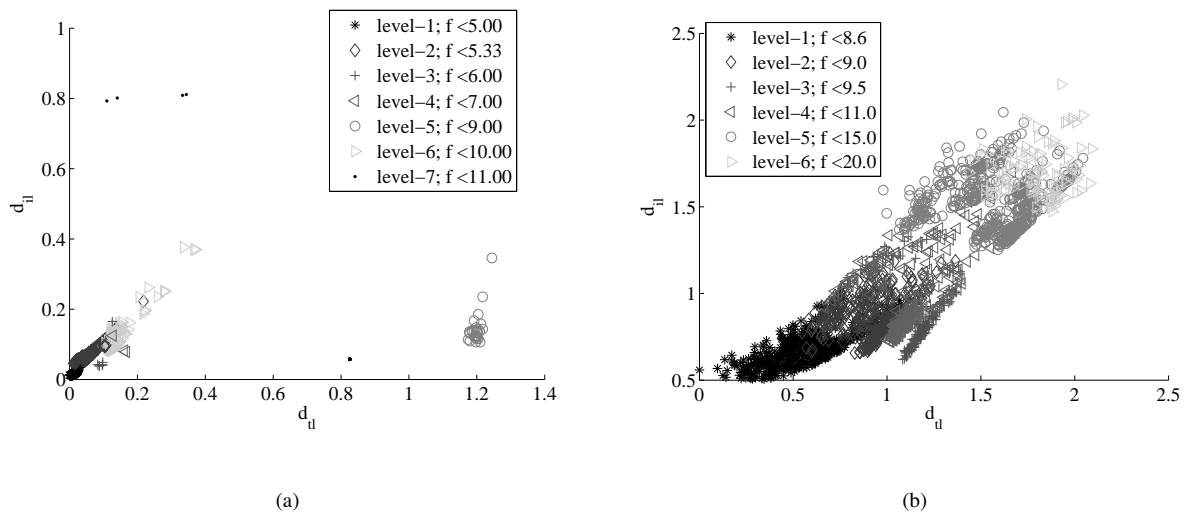
Fig. 18.   Relative distance of the local minima for Cassini: a) without DSM's and b) with DSM's.

other.

From Fig. 19 we can argue that Rosetta has a wide zone containing the global minimum together with a number of local minima with similar cost function. In fact the blue stars belonging to level 1 are distributed over values of d_{tl} in the range [0.0, 1.9] and d_{il} in the range [1.2, 1.6]. It should be noted that from a practical point of view, solutions with a difference in the total Δv of less than 50 m/s are equivalent, especially in the preliminary design phase of a mission. Therefore, all the blue stars belonging to level 1 are potentially good candidates for a space mission. Note that, the solutions at level 1 are very far apart. Thus, a transition within this group and the identification of the global minimum can be problematic.

In addition to the solutions at level 1, the search space of Rosetta presents two interesting groups at level 3 and level 4. These two sets of local minima have a relatively low inter-distance d_{il} but are far from the global minimum, since d_{tl} is quite high. They represent two strong attractors that explain why, for example, the actual Rosetta mission has a total Δv a bit higher than 1.7 km/s.

The Messenger mission problem presents a different structure, see Fig. 20. The structure of the search space of the Messenger test case appears to be characterized by many small basins separated from one another. Even the level under the threshold adopted to compute the success rate contains two distinct, yet similar, regions.

VII. CONCLUSION

In this paper we casted an evolutionary heuristic in the form of a discrete map. The discrete map can be seen as a variant of Differential Evolution. We then demonstrated empirically and theoretically that the map has a number of fixed points to which it converges asymptotically under some assumptions on the structure of the search space. This result suggested the development of an algorithm that outperforms Differential Evolution on some difficult space
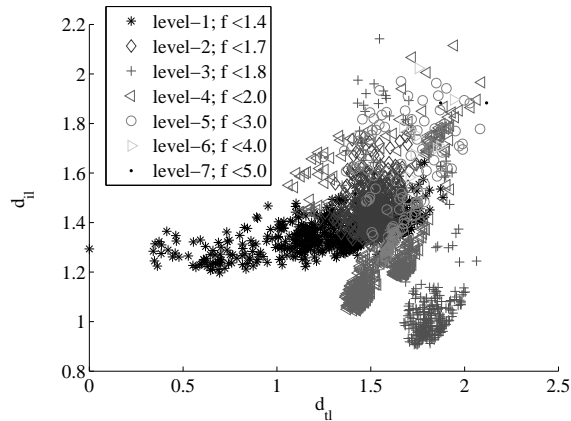
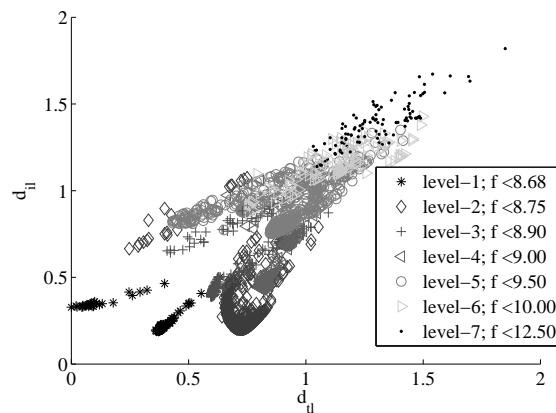Fig. 19.   Relative distance of the local minima for Rosetta

Fig. 20.   Relative distance of the local minima for Messenger

trajectory design problems. The novel algorithm displays a remarkable robustness, i.e., the ability to repeatedly converge to solutions with a value of the cost function close to the best known solution to date. Furthermore, it shows the desirable characteristic of increasing its performance with the number of function evaluations, reaching in some cases success rates which are up to around 25 times higher than the standard DE. These considerations can be generalized to all problems with similar characteristics of the search space.

VIII. ACKNOWLEDGMENTS

REFERENCES

[1] M. Clerc and J. Kennedy, "The particle swarm – explosion, stability, and convergence in a multidimensional complex space," *IEEE Transactions on Evolutionary Computation*, vol. 6, no. 1, pp. 58 – 73, 2002.

[2] I. C. Trlea, "The particle swarm optimization algorithm: convergence analysis and parameter selection," *Information processing letters*, vol. 85, pp. 317 – 325, 2003.

[3] M. Clerc, *Particle Swarm Optimization*. ISTE, 2006.

[4] R. Poli, "Dynamics and stability of the sampling distribution of particle swarm optimisers via moment analysis," *Journal of Artificial Evolution and Applications*, 2008.

[5] K. Price, R. Storn, and J. Lampinen, *Differential Evolution. A Practical Approach to Global Optimization*, ser. Natural Computing Series. Springer, 2005.

[6] M. Dellnitz, O. Schutze, and S. Sertl, "Finding zeros by multilevel subdivision techniques," *IMA Journal of Numerical Analysys*, vol. 22, pp. 167–185, 2002.

[7] A. Prügel-Bennett, "Dynamics and stability of the sampling distribution of particle swarm optimisers via moment analysis," *Journal of Theoretical Biology*, vol. 185, pp. 81–95, Mar 1997.

[8] A. Prügel-Bennett and A. Rogers, "Modelling GA dynamics," in *Theoretical Aspects of Evolutionary Computing, Natural Computing*, L. Kallel, B. Naudts, and A. Rogers, Eds. Springer, 2001, pp. 59–86.

[9] H. G. Beyer, "On the dynamics of EAs without seletion," in *Foundations of Genetic Algorithms 5*, W. Banzhaf and C. Reeves, Eds. San Francisco, CA: Morgan Kaufmann Publisher, 1998.

[10] S. Sertl and M. Dellnitz, "Global optimization using a dynamical systems approach," *Journal of Global Optimization*, vol. 34, no. 4, pp. 569–587, 2006.

[11] R. Storn and K. Price, "Differential evolution - a simple and efficient heuristic for global optimization over continuous spaces," *Journal of Global Optimization*, vol. 11, pp. 341–359, 1997.

[12] R. H. Leary, "Global optimization on funneling landscapes," *Journal of Global Optimtisation*, vol. 18, pp. 367–383, 2000.

[13] R. T. Rockafellar, *Convex analysis*. Princeton University Press, 1970.

[14] D. J. Wales and J. P. K. Doye, "Global optimization by basin-hopping and the lowest energy structures of lennard-jones clusters containing up to 110 atoms," *Journal of Physical Chemistry A*, vol. 101, pp. 5111–5116, July–August 1997.

[15] M. Locatelli, "On the multilevel structure of global optimization problems," *Computational Optimization and Applications*, vol. 30, pp. 5–22, 2005.

[16] F. Peng, K. Tang, G. Chen, and X. Yao, "Multi-start jade with knowledge transfer for numerical optimization," in *Proceedings of the 2009 IEEE Congress on Evolutionary Computation (CEC2009)*, Trondheim, Norway, May 2009.

[17] F. Neri and V. Tironnen, "Recent advances in differential evolution: a survey and experimental analysis," *Artificial Intelligence Reviews*, vol. 33, pp. 61–106, 2010.

[18] A. Auger and N. Hansen, "A restart cma evolution strategy with increasing population size," in *Proceedings of the 2005 IEEE Congress on Evolutionary Computation (CEC2005)*, Edinburgh, Scotland, UK, September 2005.

[19] M. Sentinella, "Comparison and integrated use of differential evolution and genetic algorithms for space trajectory optimisation," in *Proceedings of the 2007 IEEE Congress on Evolutionary Computation (CEC2007)*, Singapore, September 2007.

[20] J. Pinter, "Convergence properties of stochastic optimization procedures," vol. 15, no. 3, pp. 405–427, 1984.

[21] G. Rudolph, "Convergence of evolutionary algorithms in general search space," in *Proceedings of the IEEE International Conference on Evolutionary Computation*, Nagoya, Japan, May 1996.

[22] R. Battin, *An Introduction to the Mathematics and Methods of Astrodynamics*. AIAA, 1999.

[23] D. R. Myatt, V. Becerra, S. Nasuto, and J. Bishop, "Global optimization tools for mission analysis and design," ESA/ESTEC, Final Rept. ESA Ariadna ITT AO4532/18138/04/NL/MV,Call03/4101, 2004.

[24] M. Vasile and P. De Pascale, "Preliminary design of multiple gravity-assist trajectories," *Journal of Spacecraft and Rockets*, vol. 43, no. 4, pp. 5–22, July–August 2006.

[25] B. Addis, M. Locatelli, and F. Schoen, "Local optima smoothing for global optimization," *Optimization Methods and Software*, vol. 20, pp. 417–437, 2005.

[26] M. Vasile, E. Minisci, and M. Locatelli, "Analysis of some global optimization algorithms for space trajectory design," *AIAA Journal of Spacecraft and Rockets*, vol. 47, pp. 334–344, 2010.

[27] C. J. Adcock, "Sample size determination: a review," *The Statistician*, vol. 46, no. 2, pp. 261–283, 1997.

[28] D. Zaharie, "Critical values for control parameters of differential evolution algorithm," in *Proceedings of the 2009 IEEE Congress on Evolutionary Computation (CEC2009)*, 2002.

Algorithm 1 Inflationary Differential Evolution Algorithm (IDEA)

1: Set values for n_{pop}, C_R, F, iun_{max}, and tol_{conv}, set $n_{feval} = 0$ and $k = 1$

2: Initialize $\mathbf{x}_{i,k}$ and $\mathbf{v}_{i,k}$ for all $i \in [1,...,n_{pop}]$

3: Create the vector of random values $\mathbf{r} \in U[0,1]$ and the mask $\mathbf{e} = \mathbf{r} < C_R$

4: **for all** $i \in [1,...,n_{pop}]$ **do**

5:      Select three individuals $\mathbf{x}_{i_1}, \mathbf{x}_{i_2}, \mathbf{x}_{i_3}$

6:      Create the vector $\mathbf{u}_{i,k} = \mathbf{e}[(\mathbf{x}_{i_3,k} - \mathbf{x}_{i,k}) + F(\mathbf{x}_{i_2,k} - \mathbf{x}_{i_1,k})]$

7:      $\mathbf{v}_{i,k+1} = (1 - c)\mathbf{v}_{i,k} + \mathbf{u}_{i,k}$

8:      Compute S and ν

9:      $\mathbf{x}_{i,k+1} = \mathbf{x}_{i,k} + S\nu\mathbf{v}_{i,k+1}$

10:      $n_{feval} = n_{feval} + 1$

11: **end for**

12: $k = k + 1$

13: $\rho_A = \max(\|\mathbf{x}_{i,k} - \mathbf{x}_{j,k}\|)$ for $\forall \mathbf{x}_{i,k}, \mathbf{x}_{j,k} \in P_{sub} \subseteq P_k$

14: **if** $\rho_A < tol_{conv}\rho_{A,max}$ **then**

15:      Run a local optimizer a_l from $\mathbf{x}_{best}$ and let $\mathbf{x}_l$ be the local minimum found by a_l

16:      **if** $f(\mathbf{x}_l) < f(\mathbf{x}_{best})$ **then**

17:          $f_{best} \leftarrow f(\mathbf{x}_l)$

18:      **end if**

19:      **if** $f(\mathbf{x}_{best}) < f_{min}$ **then**

20:          $f_{min} \leftarrow f(\mathbf{x}_{best})$

21:          $iun = 0$

22:      **else**

23:          $iun = iun + 1$

24:      **end if**

25:      **if** $iun \leq iun_{max}$ **then**

26:          Define a bubble D_l such that $\mathbf{x}_{best} \in D_l$ for $\mathbf{x}_{best} \in P_{sub}$ and $\forall P_{sub} \subseteq P_k$

27:          $A_g = A_g + \{\mathbf{x}_{best}\}$ where $\mathbf{x}_{best} = \arg\min_i f(\mathbf{x}_{i,k})$

28:          Initialize $\mathbf{x}_{i,k}$ and $\mathbf{v}_{i,k}$ for all $\in [1,...,n_{pop}]$, in the bubble $D_l \subseteq D$

29:      **else**

30:          Define clusters in the archive and compute the baricenter $\mathbf{x}_{c,j}$ of each cluster with $j = 1,...,n_c$.

31:          Initialize $\mathbf{x}_{i,k}$ and $\mathbf{v}_{i,k}$ for all $i \in [1,...,n_{pop}]$, in D such that $\forall i, j, \|\mathbf{x}_{i,k} - \mathbf{x}_{c,j}\| > \delta_c$

32:      **end if**

33: **end if**

34: **Termination** Unless $n_{feval} \geq n_{fevalmax}$, *goto* Step 3

Algorithm 2 Testing Procedure

1: Set to N the max number of function evaluations for A

2: Apply A to p for n times and set $j_s = 0$

3: **for all** $i \in [1, ..., n]$ **do**

4: Compute $\delta_f(\bar{\mathbf{x}}(A, i)) = \mid f_{global} - f(\bar{\mathbf{x}}(A, i)) \mid$; and $\delta_x(\bar{\mathbf{x}}(A, i)) = \|\mathbf{x}_{global} - \bar{\mathbf{x}}(A, i)\|$

5:     **if** $(\delta_f(\bar{\mathbf{x}}(A, i)) < tol_f) \wedge (\delta_x(\bar{\mathbf{x}}(A, i)) < tol_x)$ **then** $j_s = j_s + 1$

6:     **end if**

7: **end for**

LIST OF FIGURES

LIST OF TABLES